

SINGLET OXYGEN QUANTUM YIELDS OF PORPHYRIN-BASED PHOTSENSITIZERS FOR PHOTODYNAMIC THERAPY

BU-HONG LI*, LI-SHENG LIN, HUI-YUN LIN
and SHU-SEN XIE

*Key Laboratory of OptoElectronic Science and
Technology for Medicine, Fujian Normal University
Ministry of Education, Fuzhou
Fujian 350007, China
bhli@fjnu.edu.cn

The major cytotoxic agent with most current photosensitizers used in photodynamic therapy (PDT) is widely believed to be singlet oxygen ($^1\text{O}_2$). Determination of the $^1\text{O}_2$ quantum yields for porphyrin-based photosensitizers, including hematoporphyrin derivative (HiPorfin), hematoporphyrin monomethyl ether (HMME) and photodynamic therapy (PsD-007) in air-saturated dimethylformamide (DMF) solutions were performed by the direct measurement of their near-infrared luminescence. In addition, $^1\text{O}_2$ quencher sodium azide was employed to confirm the $^1\text{O}_2$ generation from the investigated photosensitizers. The maximal $^1\text{O}_2$ luminescence occurs at about 1280 nm with full width at half maximum of 30 nm. The $^1\text{O}_2$ quantum yields were found to be 0.61 ± 0.03 , 0.60 ± 0.02 and 0.59 ± 0.03 for HiPorfin, HMME and PsD-007, respectively. These results provide that these porphyrin-based photosensitizers produce $^1\text{O}_2$ under irradiation, which is of significance for the study of their photodynamic action in PDT.

Keywords: Photodynamic therapy; porphyrin; singlet oxygen; luminescence; quantum yield.

1. Introduction

Photodynamic therapy (PDT) is a promising treatment modality for selective destruction of both oncologic and nononcological diseases that involves the simultaneous presence of light, photosensitizer and oxygen to achieve cytotoxic effect.^{1–3} Photofrin, a complex mixture of porphyrin oligomers has firstly received FDA approval for clinical PDT, but its photodynamic and toxicity profiles are far from ideal. As a result, a large number of porphyrin-based photosensitizers have been reported since the introduction of Photofrin, with the aim to identify agents with more favorable characteristics.^{4–8} PDT was started in the People's

*Corresponding author.

Republic of China in the early 1980s after domestically produced hematoporphyrin derivative (HpD) became available. Since then, numerous new porphyrin-based photosensitizers have been also synthesized and evaluated.^{9–10} Several promising ones have undergone clinical investigations and a few have entered into formal clinical trials, such as hematoporphyrin monomethyl ether (HMME), photocarcinorin (PsD-007), second-generation hematoporphyrin derivative (HiPorfin), and 5-ALA (Aminolevulinic acid hydrochloride for topical powder). Among them, HiPorfin and 5-ALA have recently obtained Chinese State Food and Drug Administration (SFDA) regulatory approval for applications in clinical PDT.

It is widely believed that the mechanism of PDT is based on the interaction between the excited photosensitizer and surrounding oxygen molecules, generating reactive oxygen species, particularly singlet oxygen ($^1\text{O}_2$) that resulting in irreversible damage of the target tissues.^{11–13} We have shown recently that the cell survival correlated well with cumulative $^1\text{O}_2$ for ALA-induced PpIX and exogenous PpIX based PDT.¹⁴ Thus, the $^1\text{O}_2$ generation is extremely crucial to the success of PDT, and one of the first tests performed on potential photosensitizers is to determine their $^1\text{O}_2$ quantum yields.^{15–17} Unfortunately, the $^1\text{O}_2$ quantum yields of porphyrin-based photosensitizers used in China, mainly including HiPorfin, HMME and PsD-007 have not yet determined. The methodology or technique used to measure $^1\text{O}_2$ quantum yield for photosensitizers ranges from direct detection of the luminescence produced on relaxation of steady-state or time-resolved near-infrared (NIR) $^1\text{O}_2$ luminescence, calorimetric techniques (photoacoustic calorimetry and time-resolved thermal lensing), quantitative analysis of photooxidation reactions (oxygen uptake or loss of absorbance or fluorescence of a specific probe) and enzyme inhibition.¹⁸ In comparison to the indirect methods, the direct detection of $^1\text{O}_2$ emission in the NIR region of the spectrum is commonly considered the most accurate determination of $^1\text{O}_2$ quantum yields.^{8,19} The goal of the present study is to investigate the $^1\text{O}_2$ generation from HiPorfin, HMME and PsD-007 in air-saturated DMF solutions, and to determine their $^1\text{O}_2$ quantum yields by the direct detection of NIR $^1\text{O}_2$ luminescence.

2. Materials and Methods

Chemicals. HiPorfin (5 mg/mL) was purchased from Chongqing Huading Modern Biopharmaceutics Co., Ltd. (Chongqing, China). HMME and PsD-007 were provided by Honglv Photosensitizer Co., Ltd. (Shanghai, China). Rose bengal (RB) and sodium azide (NaN_3) were obtained from Sigma (Sigma-Aldrich., St. Louis, USA). Dimethylformamide (DMF, purity, $\geq 99.5\%$) was obtained from Tianjin BASIFU Chemical Trade Co., Ltd. (Tianjin, China). The chemicals were used as received. Stock solutions of 0.1 mM the porphyrin-based photosensitizers and RB were prepared by dissolving in DMF, and the stock was stored in the dark at 4°C until needed. Preparation was done in near dark conditions to prevent photosensitized degradation of the sensitizer.

Absorption spectroscopy. The absorption spectra of all samples between 300 and 700 nm with 1 nm resolution were measured at room temperature using a Perkin Elmer Lambda 950 UV/Vis/NIR Spectrophotometer (Waltham, MA, USA). The solutions were placed in a standard 10 mm pathlength quartz cuvette (Yixing Jingke Optical Instrument Co., Ltd., Yingxing, Jiangsu, China) for measurement. In order to minimize inner-filter effects, all samples have an absorbance within 0.2 at the selective excitation wavelength were prepared for $^1\text{O}_2$ luminescence measurements.

$^1\text{O}_2$ luminescence measurement. The $^1\text{O}_2$ luminescence spectra of all samples from 1240 to 1320 nm with 1 nm step were recorded perpendicularly to the excitation beam on a commercial FLS920 spectrofluorimeter (Edinburgh Instruments Ltd., UK), which equipped with a 450-W xenon arc lamp. All samples, containing 2.5 mL solution was held in a quartz cuvette mounted on a VARIOMAG magnetic stirrer unit (MINI, H+P Labortechnik AG, Bayern, Germany). This allowed the samples to be continuously stirred with a magnetic stirring bar and maintained the source-sample-detector geometry constant between experiments. The cuvette was open so that the solutions were exposed to room air at the top. A NIR cut-off filter (HWB850, Jiangsu Haiian Huihong Photoelectric Instrument Co., Ltd., Haiian, Jiangsu, China) was placed before the entrance slit of the emission monochromator in order to block any emission under 850 nm. The weak $^1\text{O}_2$ luminescence is detected by a high-sensitive NIR photomultiplier (R5509-72, Hamamatsu Corp., Bridgewater, NJ, USA) at an operating voltage of -1600 V , which supplied with cooled housing with nitrogen flow cooling system for temperature control of -80°C . The $^1\text{O}_2$ luminescence spectra were recorded with excitation and emission bandwidths of 18 nm, and the signal integration time was 1.0 s. The wavelength dependence of the excitation power and the detector response was auto-corrected and calibrated for all $^1\text{O}_2$ emission spectra.

$^1\text{O}_2$ quantum yield determination. The determination of the $^1\text{O}_2$ quantum yields was based on the direct detection of NIR $^1\text{O}_2$ luminescence. The basic principle of this approach is to measure the intensity of the photosensitized generated steady-state $^1\text{O}_2$ luminescence around its emission peak upon continuous excitation. The $^1\text{O}_2$ luminescence intensity then can be described by the following equation¹⁹

$$I = \gamma \cdot K_T \cdot \tau_\Delta \cdot \Phi_\Delta \cdot I_{ex} \cdot A_{ex} \quad (1)$$

where γ is a constant factor given by the measurement setup, K_T is the rate constant of radiative transitions of $^1\text{O}_2$ luminescence, τ_Δ is the $^1\text{O}_2$ lifetime, Φ_Δ is the $^1\text{O}_2$ quantum yield to be calculated, I_{ex} and A_{ex} are the intensity and the absorbance for the incident excitation light.

The $^1\text{O}_2$ luminescence intensity in DMF should only depend on γ , τ_Δ , Φ_Δ , I_{ex} , and A_{ex} . γ and I_{ex} depend on the experimental setup, and can fully be controlled and kept constant. $^1\text{O}_2$ quantum yield determinations based on the above method require the use of a reference sensitizer. In this study, RB, whose $^1\text{O}_2$ quantum

yield is well known was used as a reference. Therefore, the intensities of $^1\text{O}_2$ luminescence of photosensitizer and RB can be compared directly with each other. The determination of Φ_{Δ} reduces to

$$\Phi_{\Delta} = \frac{I/A}{I_{RB}/A_{RB}} \cdot \frac{\tau_{\Delta RB}}{\tau_{\Delta}} \cdot \Phi_{\Delta RB} \quad (2)$$

where the index “RB” indicates rose bengal, I and I_{RB} are the $^1\text{O}_2$ luminescence intensity, A and A_{RB} are the absorbance, τ_{Δ} and $\tau_{\Delta ref}$ are the $^1\text{O}_2$ lifetimes, and $\Phi_{\Delta RB}$ (0.47) is the $^1\text{O}_2$ quantum yield of RB in DMF.¹⁸ This equation is valid when the photobleaching effects can be neglected.

3. Results and Discussion

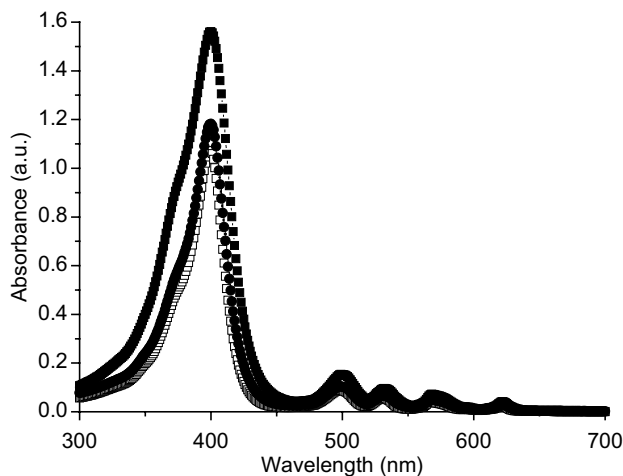
Absorption spectra. The UV-visible absorption spectra of HiPorfin, HMME and PsD-007 in DMF are shown in Fig. 1(a). The absorption spectra are very similar to that of traditional PDT drug Photofrin, with a Soret peak at 400 nm. Figure 1(b) presents the typical linear absorption spectra of HiPorfin, and the absorbance at 400 nm is linearly dependent on concentration in the range of 2.5 to 15 μM (see the inset). The spectra exhibit no concentration-induced changes in the spectra positions and shapes of absorption bands, which exclude any HiPorfin aggregation within this concentration range. This is confirmed by the absence of any shift in the fluorescence spectra (data not shown). This lack of aggregation is extremely important for the determination of $^1\text{O}_2$ quantum yield as aggregated photosensitizers lead to a strong decrease in $^1\text{O}_2$ luminescence intensity.⁴

Selection of excitation wavelength for $^1\text{O}_2$ luminescence measurement.

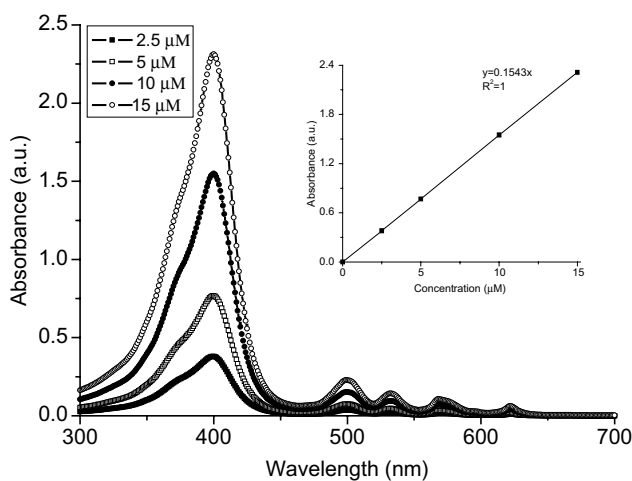
As shown in Fig. 2, there has an overlap at 506 nm for the absorption spectra of HiPorfin and RB. In order to achieve a maximal absorption for both HiPorfin and RB, the excitation wavelength was set to 506 nm for the following $^1\text{O}_2$ luminescence measurements.

$^1\text{O}_2$ luminescence of porphyrin-based photosensitizers. High efficiency of $^1\text{O}_2$ generation from HiPorfin, HMME, PsD-007, and RB in air-saturated DMF was detected, an example of which is presented in Fig. 3, showing the typical $^1\text{O}_2$ luminescence spectra of HiPorfin. The maximal emission peak of $^1\text{O}_2$ luminescence lies around 1280 nm with full width at half maximum of 30 nm, which is consistent with the literature values.^{20,21} Its position and shape independent of concentration, while the $^1\text{O}_2$ luminescence intensity at 1280 nm was linearly dependent on HiPorfin concentration, as expected. No spectral shift of $^1\text{O}_2$ luminescence spectra was observed for HiPorfin, HMME, PsD-007 and RB (data not shown).

Confirmation that the detected signal was due to $^1\text{O}_2$ luminescence was achieved by added NaN_3 , a specific chemical $^1\text{O}_2$ quencher, resulted in elimination of $^1\text{O}_2$ luminescence. To investigate this, additional NaN_3 was rapidly added to the solution after $^1\text{O}_2$ luminescence measurement, and then the second spectroscopy was continuously recorded for comparison. As illustrated in Fig. 4, the $^1\text{O}_2$ luminescence



(a)



(b)

Fig. 1. (a) Absorption spectra of HiPorfin (■), HMME (□) and PsD-007 (●) in DMF, and the concentrations were $10 \mu\text{M}$, (b) absorption spectra of HiPorfin in DMF, and the concentrations varied from 2.5 to $15 \mu\text{M}$. Concentration dependence of HiPorfin absorbance at 400 nm is shown in the insert.

intensity of HiPorfin dramatically decreased after added various amount of NaN_3 . The observed depletion is attributed to the reaction of NaN_3 with sensitized $^1\text{O}_2$.

$^1\text{O}_2$ quantum yields of porphyrin-based photosensitizers. As shown in Fig. 5, the $^1\text{O}_2$ luminescence intensities of HiPorfin, HMME, PsD-007 and RB show a linear dependence on their absorbance, as expected. The data give an excellent fit to a straight line with zero intercept, and the slope of the line is

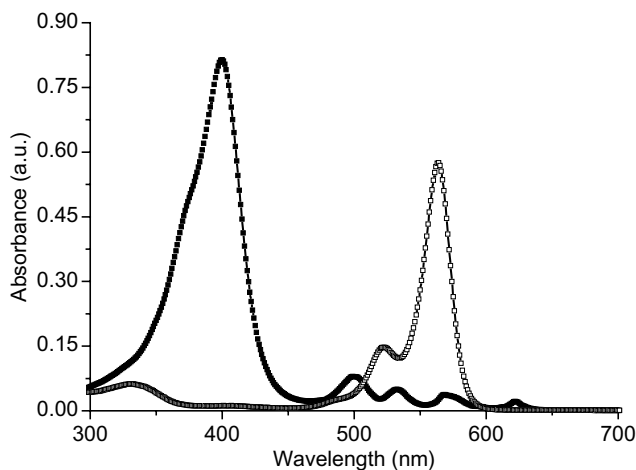


Fig. 2. Absorption spectra of HiPorfin (■) and RB (□) in DMF. The HiPorfin and RB concentrations were $5 \mu\text{M}$.

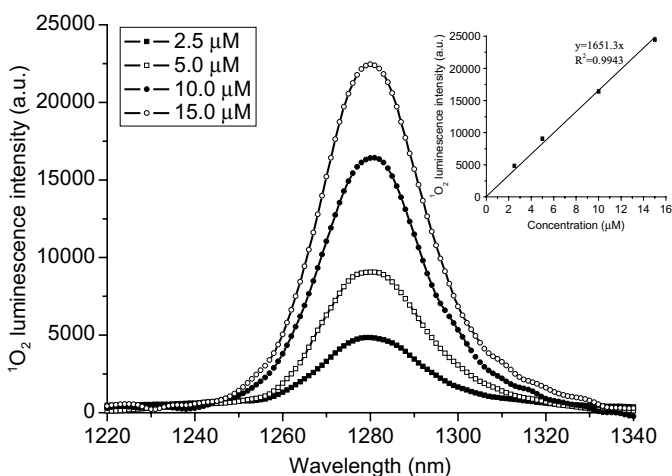


Fig. 3. $^1\text{O}_2$ luminescence spectra for HiPorfin in DMF, for an excitation wavelength is 506 nm. Concentration dependence of $^1\text{O}_2$ luminescence intensity at 1280 nm is indicated in the insert.

predicted by the computer fit. The $^1\text{O}_2$ lifetimes for HiPorfin, HMME, PsD-007 and RB have a very similar value of $19.2 \pm 0.8 \mu\text{s}$ in DMF, which were deduced from fitting of the time-resolved $^1\text{O}_2$ luminescence spectra at 1280 nm (data not shown). The determination $^1\text{O}_2$ quantum yields were performed for three independent measurements with a maximum standard deviation of 5%. Porphyrin-based photosensitizers are widely considered to have high $^1\text{O}_2$ production.⁸ This is also demonstrated in this study. The $^1\text{O}_2$ quantum yields were found to be 0.61 ± 0.03 , 0.60 ± 0.02 and 0.59 ± 0.03 for HiPorfin, HMME and PsD-007, respectively, as

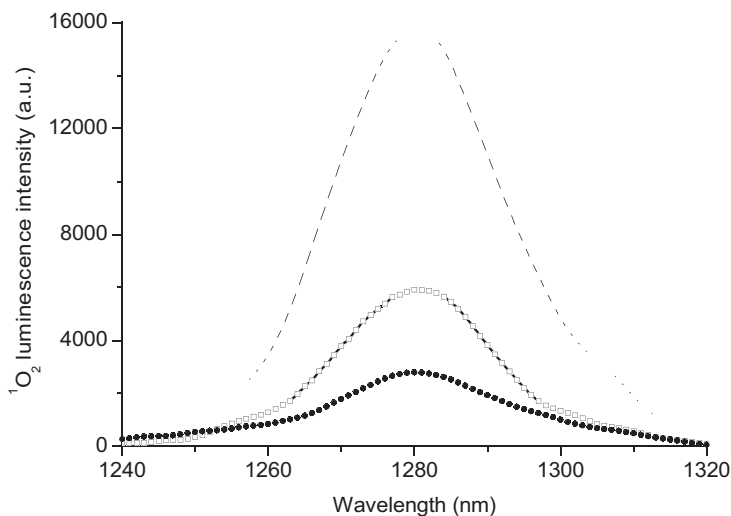


Fig. 4. Quenching of $^1\text{O}_2$ luminescence of HiPorfin in DMF by NaN_3 . The HiPorfin concentrations were $10\ \mu\text{M}$, while the final NaN_3 concentrations in the solutions were 10 (\square) and 40 (\bullet) μM , respectively.

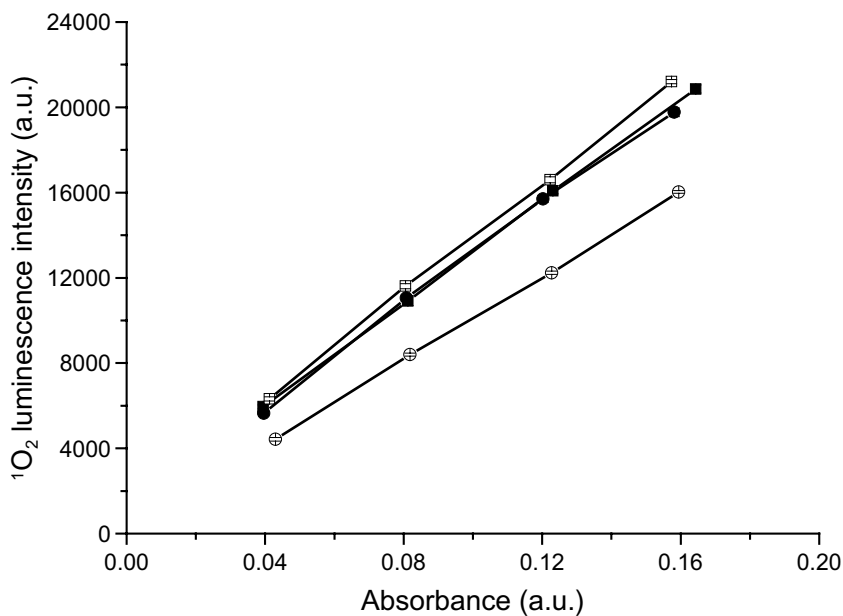


Fig. 5. Plot of $^1\text{O}_2$ luminescence counts against the absorbance for HiPorfin (\blacksquare), HMME (\square), PsD-007 (\bullet), and RB (\circ) in DMF, respectively. The $^1\text{O}_2$ luminescence counts were measured at $1280\ \text{nm}$. The error bars represent the standard deviation of the mean of three independent experiments.

calculated using Eq. (2). These values are in excellent agree with that reported for free base porphyrins about 0.6 and for lipophilic opp-dibenzoporphyrin (2,12-diethyl-3,13-dimethyldibenzo[g,q]porphyrin) of 0.56-0.65.^{5,7}

4. Conclusions

¹O₂ quantum yield is one of the most important parameters characterizing usefulness of the potential photosensitizers for PDT. In this study, the ¹O₂ quantum yields for the porphyrin-based photosensitizers, including HiPorfin, HMME and PsD-007 in DMF solutions have been determined by the direct measurement of their NIR luminescence. The ¹O₂ quantum yields were determined to be 0.61 ± 0.03 , 0.60 ± 0.02 and 0.59 ± 0.03 for HiPorfin, HMME and PsD-007, respectively. No significant difference in ¹O₂ quantum yields was observed. These results provide evidence that HiPorfin, HMME and PsD-007 produce ¹O₂ under irradiation, and they are typical of porphyrins with high ¹O₂ quantum yield for the promising applications in PDT.

Acknowledgements

This study was supported by the Program for New Century Excellent Talents in Fujian Province University.

References

1. D.E. Dolmans, D. Fukumura and R.K. Jain, "Photodynamic therapy for cancer," *Nat. Rev. Cancer* **3**, 380–387 (2003).
2. A. Juzeniene, Q. Peng and J. Moan, "Milestones in the development of photodynamic therapy and fluorescence diagnosis," *Photochem. Photobiol. Sci.* **6**, 1234–1245 (2007).
3. S. Verma, G.M. Watt, Z. Mai and T. Hasan, "Strategies for enhanced photodynamic therapy effects," *Photochem. Photobiol.* **83**, 96–1005 (2007).
4. A.A. Jr. Krasnovsky, K.V. Neverov, S. Yu. Egorov, B. Roeder and T. Levald, "Photophysical studies of pheophorbide a and pheophytin a. Phosphorescence and photosensitized singlet oxygen luminescence," *J Photochem. Photobiol. B.* **5**, 245–254 (1990).
5. R. Venkatesan, N. Periasamy and T.S. Srivastava, "Singlet molecular oxygen quantum yield measurements of some porphyrins and metalloporphyrins," *Proc. Indian Acad. Sci. (Chem. Sci.)* **104**, 713–722 (1992).
6. C. Tanielian, C. Schweitzer, R. Mechin and C. Wolff, "Quantum yield of singlet oxygen production by monomeric and aggregated forms of hematoporphyrin derivative," *Free Radic. Biol. Med.* **30**, 208–212 (2001).
7. S.A. Gerhardt, J.W. Lewis, J.Z. Zhang, R. Bonnett and K.A. McManus, "Photophysical behaviour of an opp-dibenzoporphyrin (2,12-diethyl-3,13-dimethyldibenzo [g,q]porphyrin) in micelles and organic solvents," *Photochem. Photobiol. Sci.* **2**, 934–938 (2003).
8. S. Mathai, T.A. Smith and K.P. Ghiggino, "Singlet oxygen quantum yields of potential porphyrin-based photosensitisers for photodynamic therapy," *Photochem. Photobiol. Sci.* **6**, 995–1002 (2007).
9. Z. Huang, "Photodynamic therapy in China: Over 25 years of unique clinical experience part one-history and domestic photosensitizers," *Photodiag. Photodyna. Ther.* **3**, 3–10 (2006).

10. D.Y. Xu, "Research and development of photodynamic therapy photosensitizers in China," *Photodiag. Photodyna. Ther.* **4**, 13–25 (2007).
11. K.R. Weishaupt, C.J. Gomer and T.J. Dougherty, "Identification of singlet oxygen as the cytotoxic agent in photoinactivation of a murine tumor," *Cancer Res.* **36**, 2326–2329 (1976).
12. M.J. Niedre, C.S. Yu, M.S. Patterson and B.C. Wilson, "Singlet oxygen luminescence as an *in vivo* photodynamic therapy dose metric: validation in normal mouse skin with topical amino-levulinic acid," *Br. J. Cancer* **92**, 298–304 (2005).
13. Y. Wei, J. Zhou, D. Xing and Q. Chen, "*In vivo* monitoring of singlet oxygen using delayed chemiluminescence during photodynamic therapy," *J. Biomed. Opt.* **12**, Art. No. 014002 (2007).
14. B.H. Li, M.T. Jarvi, E.H. Moriyama and B.C. Wilson, "Correlation between cell viability and cumulative singlet oxygen luminescence from protoporphyrin IX in varying subcellular localizations," *In Optical Methods for Tumor Treatment and Detection: Mechanisms and Techniques in Photodynamic Therapy XVI* Vol. 6427 (Edited by D. Kessel), Art. No. 642707. The International Society for Optical Engineering, San Jose, CA (2007).
15. K.D. Belfield, C.C. Corredor, A.R. Morales, M.A. Dessources and F.E. Hernandez, "Synthesis and characterization of new fluorene-based singlet oxygen sensitizers," *J. Fluoresc.* **16**, 105–110 (2006).
16. K.D. Belfield, M.V. Bondar and O.V. Przhonska, "Singlet oxygen quantum yield determination for a fluorene-based two-photon photosensitizer," *J. Fluoresc.* **16**, 111–117 (2006).
17. S.J. Andrasik, K.D. Belfield, M.V. Bondar, F.E. Hernandez, A.R. Morales, O.V. Przhonska and S. Yao, "One- and two-photon singlet oxygen generation with new fluorene-based photosensitizers," *ChemPhysChem* **8**, 399–404 (2007).
18. R.W. Redmond and J.N. Gamlin, "A compilation of singlet oxygen yields from biologically relevant molecules," *Photochem. Photobiol.* **70**, 391–475 (1999).
19. W. Spiller, H. Kliesch, D. Wöhrle, S. Hackbarth, B. Röder and G. Schnurpfeil, "Singlet oxygen quantum yields of different photosensitizers in polar solvents and micellar solutions," *J. Porphyrins Phthalocyanines* **2**, 145–158 (1998).
20. R. Dedic, A. Molnár, M. Kořínek, A. Svoboda, J. Pšenčík and J. Hála, "Spectroscopic study of singlet oxygen photogeneration in meso-tetra-sulphonatophenyl-porphin," *J. Lumin.* **108**, 117–119 (2004).
21. M. Kořínek, R. Dedic, A. Molnár and J. Hála, "The influence of human serum albumin on the photogeneration of singlet oxygen by meso-Tetra(4-sulfonatophenyl)porphyrin. An infrared phosphorescence study," *J. Fluoresc.* **16**, 355–359 (2006).